

# Prediction of Deflection and Stresses of Laminated Composite Plate with an Artificial Neural Network Aid

B. Sidda Reddy<sup>a\*</sup>, J. Suresh Kumar<sup>b</sup>, and K. Vijaya Kumar Reddy<sup>b</sup>

<sup>a</sup> School of Mechanical Engineering, R. G. M. College of Engineering and Technology, Nandyal, Kurnool (Dt), Andhra Pradesh, India

<sup>b</sup> Department of Mechanical Engineering, J. N. T. U. H. College of Engineering, J. N. T. University, Kukatpally, Hyderabad, India

**Abstract:** This paper discusses the use of *D*-optimal designs in the design of experiments (DOE) and artificial neural networks (ANN) in predicting the deflection and stresses of carbon fibre reinforced plastic (CFRP) square laminated composite plate subjected to uniformly distributed load. For training and testing of the ANN model, a number of finite element analyses have been carried out using *D*-optimal designs by varying the fibre orientations and thickness of each lamina. The composite plate is modeled using shell 99 elements. The ANN model has been developed using multilayer perceptron (MLP) backpropagation algorithm. The adequacy of the developed model is verified by root mean square error and regression coefficient. The results showed that the training algorithm of backpropagation was sufficient enough in predicting the deflection and stresses.

**Keywords:** *D*-optimal designs; finite element method; artificial neural networks; multilayer perceptron.

## 1. Introduction

Composite materials are particularly attractive to aviation and aerospace applications because of their exceptional strength and stiffness-to-density ratios and superior physical properties. The mechanical behavior of a laminate is strongly dependent on the fiber directions and because of that; the laminate should be designed to meet the specific requirements of each particular application in order to obtain the maximum advantages of such materials. Usually, laminated composite materials are fabricated from unidirectional plies of giving thickness and with fiber orientations limited to a small set of angles, eg.,  $0^\circ$ ,  $45^\circ$ ,  $-45^\circ$  and  $90^\circ$  [1]. A true understanding of their structural behaviour is required, such as the deflections, buckling loads and modal characteristics, the through thickness distributions of stresses and strains, the large deflection behaviour and, of extreme importance for obtaining strong, reliable multi-layered structures, the failure characteristics [2].

In the past, the structural behavior of plates and shells using the finite element method has been studied by a variety of approaches. Choudhary and Tungikar [3] analyzed the geometrically nonlinear behavior of laminated composite plates using the finite element analysis. They studied the effect of number of layers, effect of degree of orthotropy (both symmetric and antisymmetric)

---

\* Corresponding author; e-mail: [bsrrgmccet@gmail.com](mailto:bsrrgmccet@gmail.com)

Received 18 January 2013

Revised 12 March 2013

Accepted 21 May 2013

and different fibre orientations on central deflections. Ganapathi *et al.* [4] presented an eight-node  $C^0$  membrane-plate quadrilateral finite element-based on the Reissner-Mindlin plate theory to analyse moderately large deflection, static and dynamic problems of moderately thick laminates including buckling analysis and membrane-plate coupling effects. Han *et al.* [5] used the hierarchical finite element method to carry out the geometrically nonlinear analysis of laminated composite rectangular plates. Based on the first-order shear deformation theory and Timoshenko's laminated composite beam functions, the current authors developed a unified formulation of a simple displacement based 3-node, 18degree-of-freedom flat triangular plate/shell element [6] and two simple, accurate, shear-flexible displacement based 4-node quadrilateral elements [7-8] and for linear and geometrically nonlinear analysis of thin to moderately thick laminated composite plates. The deflection and rotation functions of the element boundary were obtained from Timoshenko's laminated composite beam functions. Raja Sekhara Reddy *et al.* [9] applied the artificial neural networks (ANN) in predicting the natural frequency of laminated composite plates under clamped boundary condition. They used the  $D$ -optimal design in the design of experiments to carry out the finite element analysis. WEN *et al.* [10-11] used the finite element method to predict the damage level of the materials. They studied the prediction of the elastic-plastic damage and creep damage using Gurson model and creep damage model, which is based on the Kachanov-Rabothov continuum creep damage law. They also studied the creep damage properties of thin film/substrate systems by bending creep tests and carried the Simulation of the interface characterization of thin film/substrate systems. Reddy *et al* [12] employed a distance-based optimal design in the design of experimental techniques and artificial neural networks to optimize the stacking sequence for a sixteen ply simply supported square laminated composite plate under uniformly distributed load (UDL) for minimizing the deflections and stresses using finite element method. Therefore the finite element method is especially versatile and efficient for the analysis of complex structural behavior of the composite laminated structures.

The present study proposes a new experimental design method for selection of practical laminates and thickness of each ply for a criterion of a response. This method employs  $D$ -optimality for selections from a set of feasible laminates. This method is applied to a 10 layer laminate to predict the deflection and stresses of a composite plate subjected to a uniform distributed load under simply supported boundary condition and an artificial neural network model has been developed to predict the same.

## 2. Material and methods

The material used to model the physical structure of the laminated composite plate is carbon fibre reinforced plastic (CFRP). The material properties are as follows [13]:  
 $E_1=220GPa$ ,  $E_2=6.9GPa$ ,  $E_3=6.9GPa$ ,  $G_{12}=G_{23}=G_{13}=4.8GPa$ ,  $\nu_{12}=0.25$ ,  $\nu_f=0.6$ .

The methodology adopted in predicting the deflections and stresses using the integrated approach is shown in Figure 1.

### 2.1. Geometry of the shell 99 element

In this study to model the laminated composite plate the finite element analysis software ANSYS has been used. In ANSYS software, there are many element types available to model layered composite materials. In our FE analysis, the linear layered structural shell element (Shell 99) is used. It is designed to model thin to moderately thick plate and shell structures with a

side-to-thickness ratio of roughly 10 or greater. The linear layered structural shell element allows a total of 250 uniform-thickness layers. Alternatively, the element allows 125 layers with thicknesses that may vary bilinearly over the area of the layer. An accurate representation of irregular domains (i.e. domains with curved boundaries) can be accomplished by the use of refined meshes and/or irregularly shaped elements. For example, a non-rectangular region cannot be represented using only rectangular elements; however, it can be represented by triangular and quadrilateral elements. Since, it is easy to derive the interpolation functions for a rectangular element, and it is much easier to evaluate the integrals over rectangular geometries than over irregular geometries, it is practical to use quadrilateral elements with straight or curved side assuming you have a means to generate interpolation functions and evaluate their integrals over the quadrilateral elements [14-15]. The linear layered structural shell element is shown in Figure 2. Nodes are represented by I, J, K, L, M, N, O, and P.

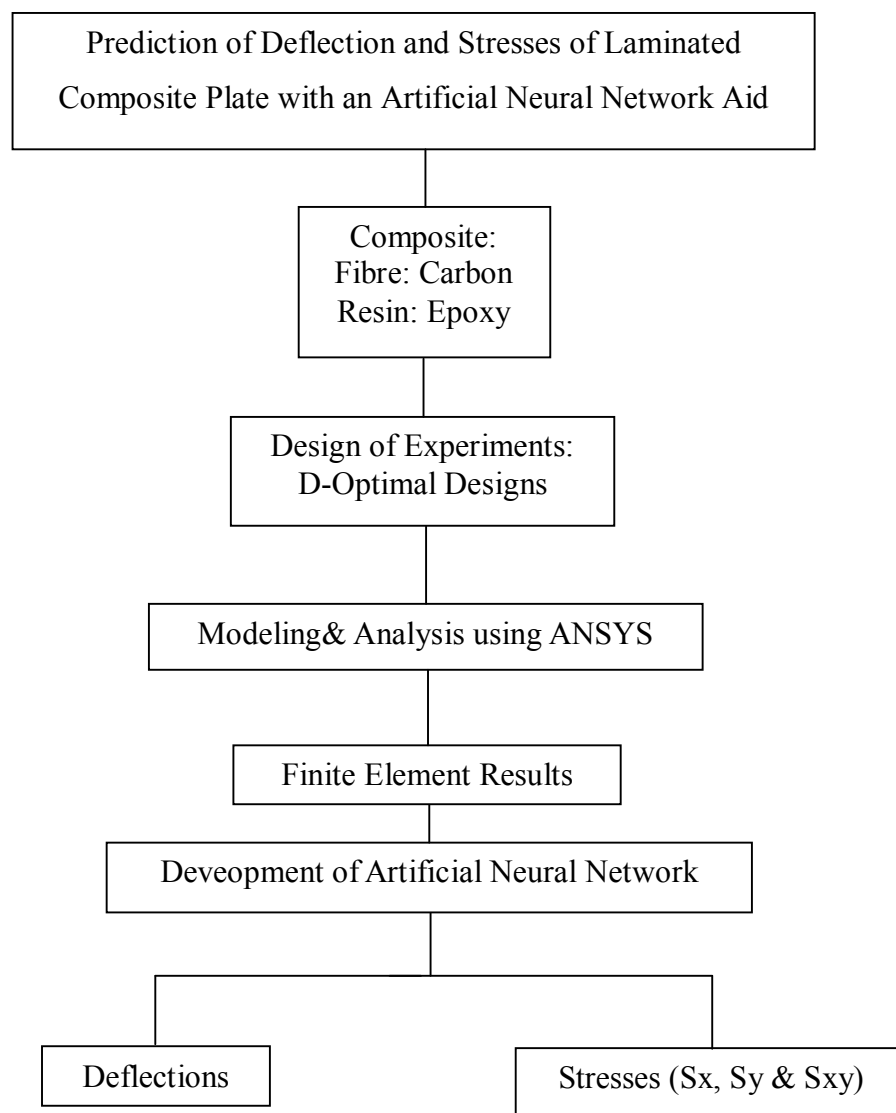


**Figure 1.** Generic model

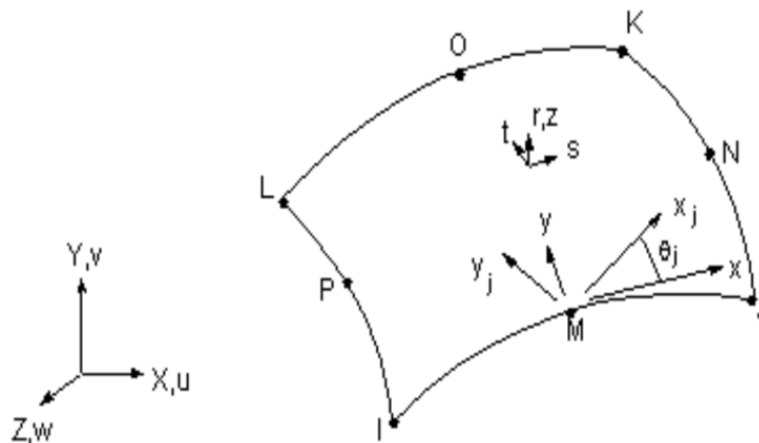


**Figure 2.** Geometry of 8-node element with six degrees of freedom

## 2.2. Design of experiments

Design of Experiments (DOE) is a mathematical methodology that defines an optimal set of experiments in the design space, in order to obtain the most relevant information possible with the highest accuracy at the lowest cost. This scientific exploration of the design space replaces a tedious, manual, trial-and-error process, and is the fastest way to acquire the most relevant information with minimum computational effort. Traditional experimental designs (Full Factorial Designs, Fractional Factorial Designs, and Response Surface Designs) are appropriate for calibrating linear models in experimental settings where factors are relatively unconstrained in the region of interest. In some cases, however, models are necessarily nonlinear. In other cases, certain treatments (combinations of factor levels) may be expensive or infeasible to measure. D-optimal designs are model-specific designs that address these limitations of traditional designs.

The *D*-optimality criterion states that the best set of points in the experiment maximizes the determinant  $|X^T X|$ . "D" stands for the determinant of the X matrix associated with the model. A *D-optimal* design is generated by an iterative search algorithm and seeks to minimize the covariance of the parameter estimates for a specified model. This is equivalent to maximizing the determinant  $D=|X^T X|$ , where X is the design matrix of model terms (the columns) evaluated at specific treatments in the design space (the rows). Unlike traditional designs, *D-optimal* designs do not require orthogonal design matrices, and as a result, parameter estimates may be correlated. Parameter estimates may also be locally, but not globally, *D-optimal*. The *D-optimal* design uses the row-exchange and Co-ordinate exchange algorithms to generate the optimal designs [16].

A related measure of the moment matrix ( $X^T X/k$ ) is the *D*-efficiency and can be calculated by using the following expression:

$$D - efficiency = 100 \left( \frac{1}{N_D} |X^T X|^{1/p} \right) \quad (1)$$

where

$N_D$  is the number of points in the design and  $p$  is the number of effects in the model including the intercept. If all variables are normalized so that they vary from -1 to 1, then the maximum value of the  $D_{eff}$  is 1. Furthermore, the quality of the set of points can then be measured by  $D_{eff}$ .

### 2.3. Artificial neural networks

An Artificial Neural Network (ANN) is an information processing paradigm that is inspired by the way biological nervous systems, such as the brain, process information. It resembles the human brain in two aspects: the knowledge is acquired by the network through a learning process, and inter neuron connection strengths known as synaptic weights are used to store the knowledge. A typical biological neuron collects signals from others through a host of fine structures called dendrites. The neuron sends out spikes of electrical activity through a long, thin strand known as an axon, which splits into thousands of branches. At the end of each branch, a structure called a synapse converts the activity from the axon into electrical effects that inhibit or excite activity from the axon into electrical effects that inhibit or excite activity in the connected neurons. When a neuron receives excitatory input that is sufficiently large compared with its inhibitory input, it sends a spike of electrical activity down its axon. Learning occurs by changing the effectiveness of the synapses so that the influence of one neuron on other changes. A biological neuron and artificial neuron are shown in Figure 3 and Figure 4 respectively.

The analogy of biological neuron to artificial neuron is as follows:

Human	Artificial
Neuron	Processing Element
Dendrites	Combining Function
Cell Body	Transfer Function
Axons	Element Output
Synapses	Weights

The use of artificial neural networks (ANN) has been well accepted in the areas of telecommunication, signal processing, pattern recognition, prediction, process control and financial analysis. Neural networks are built by connecting these neurons together by weighted interconnections. The determination of these weights called training is the most significant task. In supervised learning the network is trained to learn a mapping from certain inputs to given outputs. An example of supervised learning is the back propagation method for multilayer perceptron (MLP) networks. Multilayer means the addition of one or more hidden layers in between the input and output layers. In the network each neuron receives total input from all of the neurons in the preceding layer according to the Eq. (2).

$$net_j = \sum_{i=0}^N W_{ij} X_i \tag{2}$$

Where  $net_j$  is the total or net input and  $N$  is the number of inputs to the  $j^{th}$  neuron in the hidden layer.  $W_{ij}$  is the weight of the connection from the  $i^{th}$  neuron in the forward layer to the  $j^{th}$  neuron in the hidden layer. A neuron in the network produces its output ( $Out_j$ ) by processing the net input through an activation (Transfer) function, such as Tangent hyperbolic function as in Eq. (3).

$$Out_j = f(net_j) = \frac{1 - e^{-net_j}}{1 + e^{-net_j}} \tag{3}$$

In the training process the algorithm is used to calculate neuronal weights, so that the root-mean squared error between the calculated outputs and observed outputs from the training set is minimized and is calculated using Eq. (4).

$$RMSE = \left( \frac{1}{p} \sum_i |d_i - y_i|^2 \right)^{1/2} \tag{4}$$

Where  $d_i$  is the desired response (or target signal),  $y_i$  are the output units of the network, and the sums run over time and over the output units. When the root-mean square error is minimized, the power of the error (i.e. the power of the difference between the desired and the actual ANN output) is minimized.

In addition, the absolute fraction of variance ( $R^2$ ) is defined as follows:

$$R^2 = 1 - \left[ \frac{\sum_i (d_i - y_i)^2}{\sum_i (y_i)^2} \right] \tag{5}$$

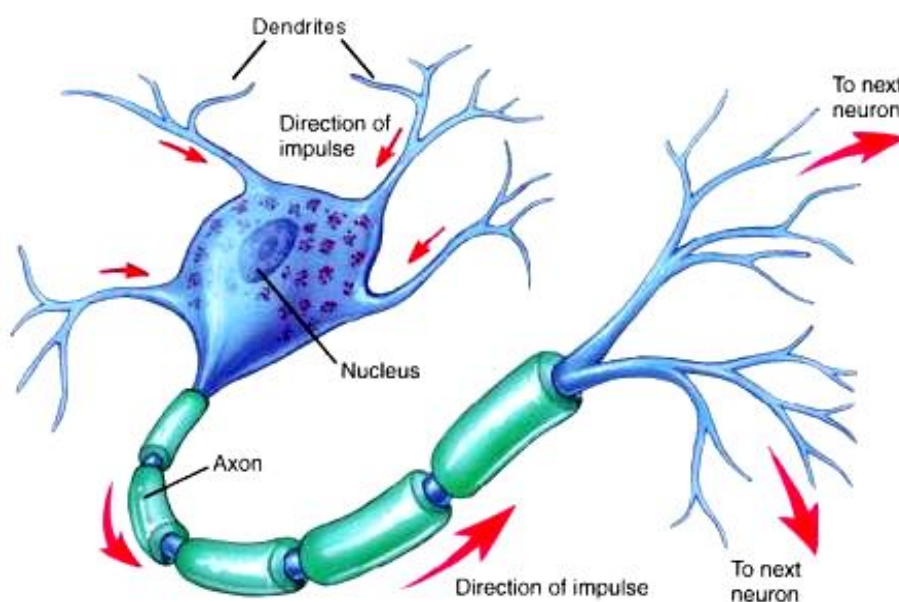


Figure 3. Simplified model of a biological neuron

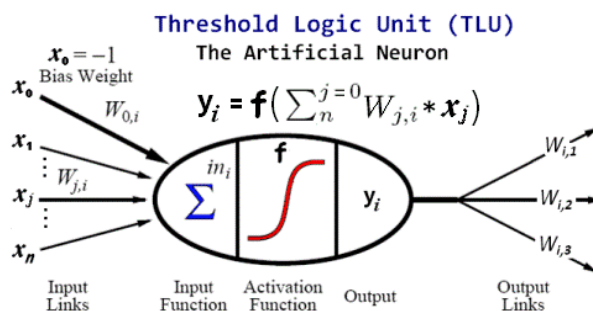


Figure 4. Artificial neuron model

### 3. Finite element analysis

#### 3.1. Validation of linear layered structural shell element-a case study

In order to validate the usage of the linear layered structural shell element, a numerical example is solved in static analysis. The boundary condition is simply supported and the geometry and material properties are as follows:

$$E_1/E_2=40, G_{12}=G_{13}=0.6E_2, G_{23}=0.5E_2, \nu_{12} = 0.25, a/h=10, a=1, q=1.0.$$

The center deflection and stresses are presented here in non-dimensional form using the following:

$$\bar{w} = w \times \frac{E_2 h^3}{qa^4} \times 10^3, \quad \bar{\sigma}_x = \sigma_x \times \frac{h}{aq}, \quad \bar{\sigma}_y = \sigma_y \times \frac{h}{aq} \quad \text{and} \quad \bar{\tau}_{xy} = \tau_{xy} \times \frac{h}{aq}$$

Table 1 and Table 2 represents the mesh convergence study and comparison of results of non-dimensional displacement obtained from Reddy [15] and the ANSYS computer program. The results using a free mesh show an excellent correlation to the results given by Reddy [15].

**Table 1.** Nondimensional displacement of composite plates (cross- ply)

Mesh	0/90	0/90/0	0/90/90/0	0/90/0/90
2 × 2	14.222	6.8178	6.5423	6.7762
4 × 4	14.478	6.9848	6.7402	6.9897
10×10	14.488	6.9904	-	6.9965
20×20	14.488	6.9905	6.7459	6.9966
40 × 40	14.475	6.9857	6.7405	6.9904
FSDT (Reddy)	14.069	6.919	6.682	6.9260
Difference (%)	2.907	0.951	0.870	0.919

**Table 2.** Nondimensional displacement of composite plates (θ/- θ/ θ/- θ)

Mesh	5	15
2 × 2	6.7716	6.3811
4 × 4	-	6.6625
10×10	6.9652	-
20×20	-	6.6668
40 × 40	6.9623	6.6631
FSDT (Reddy)	6.741	6.086
Difference (%)	3.2828	9.4824

#### 3.2. Model description

The physical structure that was used in this work is a carbon fibre reinforced plastic composite plate, shown in Figure 5. The length (a) and width (b) of the plate is 100 mm and ply orientation and thickness (h) of the plate is treated as a design variable. A total 422 analyses are performed

in this design study, using a finite element model of the plate. The model was developed using 16 linear layered structural shell elements in ANSYS 10.0. The global x-coordinate is taken along the length of the plate; the global y-coordinate is taken along the width of the plate while the global z-direction is taken out the plate surface. There are 4 elements in the axial direction and 4 along the width one. In this finite element analysis, all the sides are constrained in the Z direction only. The pressure applied to the plate is  $1\text{N/mm}^2$ .

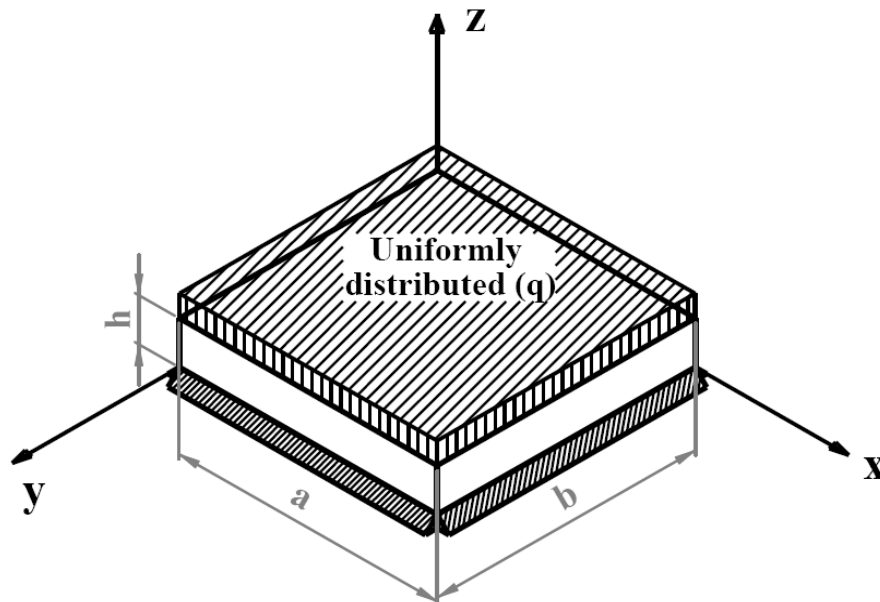


Figure 5. Uniformly loaded simply supported composite plate

### 3.3. Finite element analyses details

In the present study, the *D*-optimal design has been implemented to select a feasible set of laminates from among all feasible laminates. For the ply angle and thickness we adopt 3 levels ( $0^\circ$ ,  $45^\circ$  and  $90^\circ$ ) and 4 levels (0.2mm, 0.3mm, 0.4mm and 0.5mm) respectively for each lamina. Thus the total number of entire feasible simulations is  $3 \times 3 \times 3 \times 3 \times 3 \times 4 \times 4 \times 4 \times 4 = 2,48,832$  because we consider only a symmetric laminate and for each ply. The ‘odd’ occurrences i.e., first (outermost), third, fifth, etc. of  $45^\circ$  plies corresponds to  $45^\circ$  plies, whereas ‘even’ occurrences corresponds to  $-45^\circ$ . For example, a laminate of  $[0/45/45/90/45/0.2/0.3/0.5/0.2]$  is coded as  $[0/45/-45/90/45/0.2/0.3/0.5/0.2]$ . There is one unbalanced  $45^\circ$  ply when the number of occurrences of  $45^\circ$  plies is odd. This is repaired by replacing the  $45^\circ$  -ply with a  $90^\circ$ -ply or a  $0^\circ$ -ply. The  $45^\circ$ -ply position replaced by a  $90^\circ$ -ply or a  $0^\circ$ -ply is the innermost  $45^\circ$ -ply that can be replaced without violating the four contiguous ply rule: the same fibre angle plies must not stacked more than four plies [1]. We can select feasible laminates from the set of feasible laminates using *D*-optimal. In this study, the total 422 feasible laminates were selected for training (322 laminates), validation (80 laminates) and testing (20 laminates) of the artificial neural network model. The selected *D*-optimal set of laminates design was performed using JMP software of SAS. The material properties used throughout this study are presented in section 2. The plate is analyzed for deflections and stresses under a simply supported boundary condition when the plate is subjected to a uniformly distributed load working along the Z-direction. The variations of mean nondimensional results of the laminates are shown in Figure 6-9.



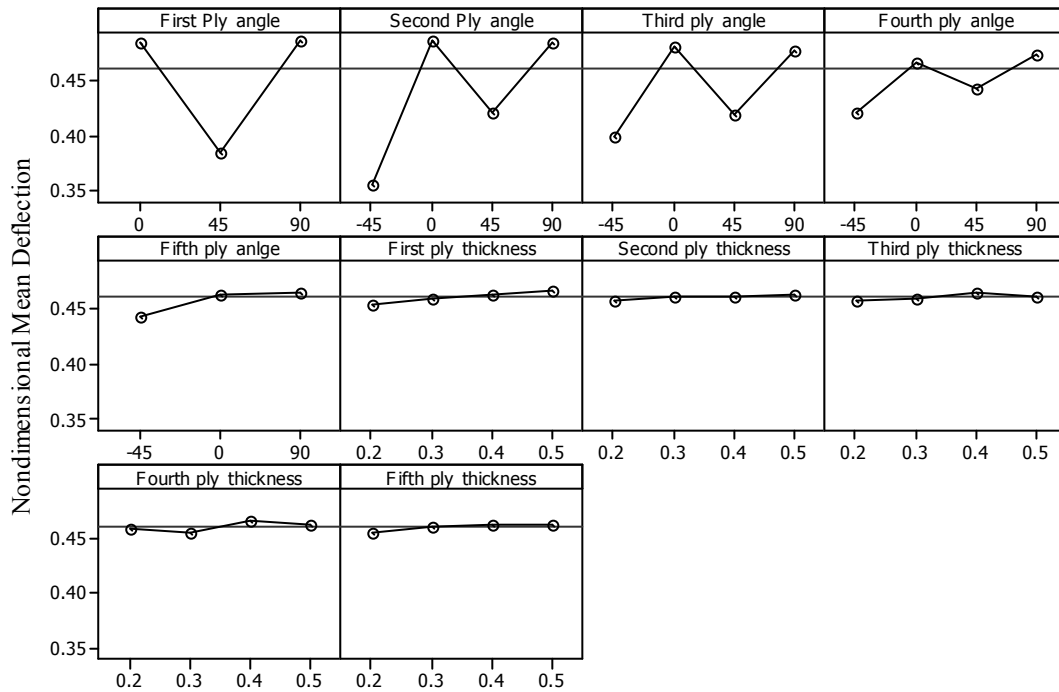


Figure 6. Variation of mean nondimensional deflection for different fibre orientations and thickness

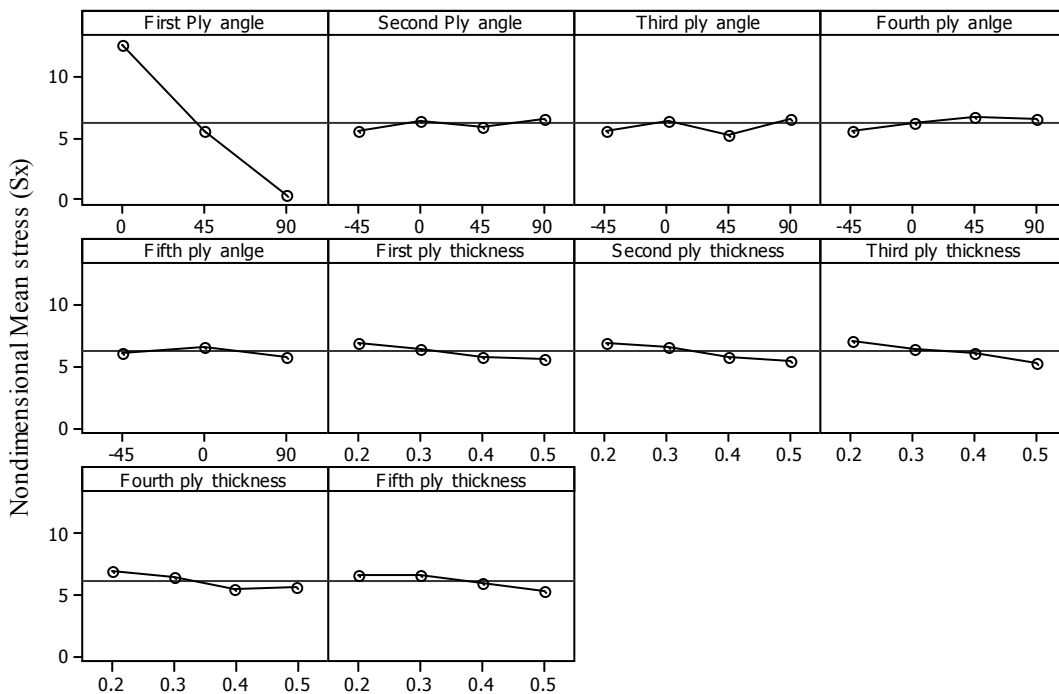
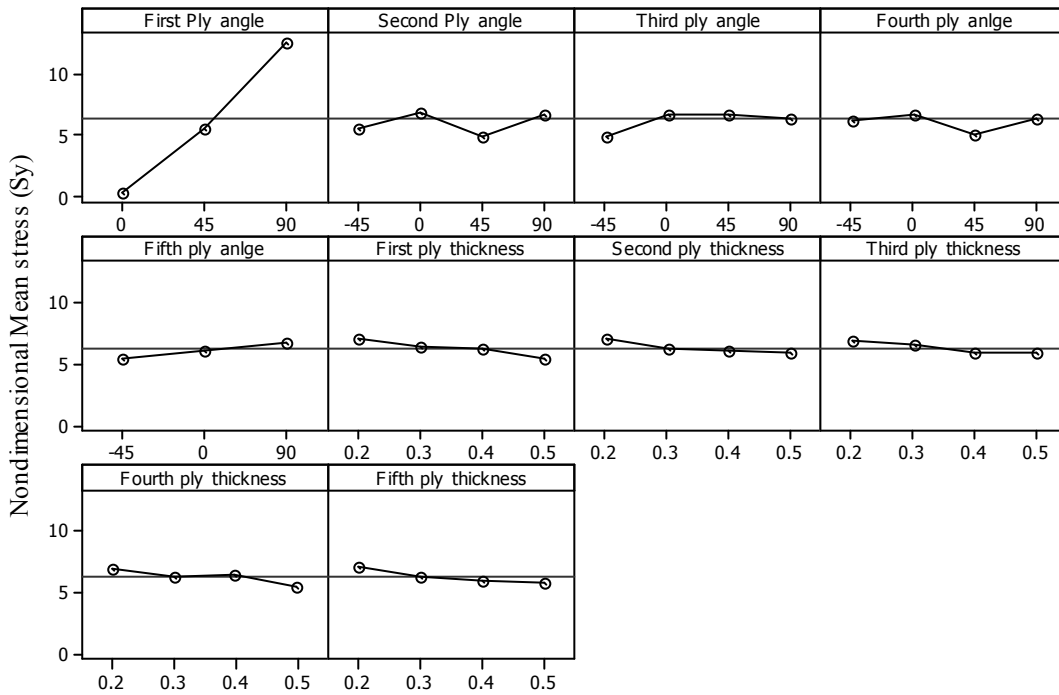
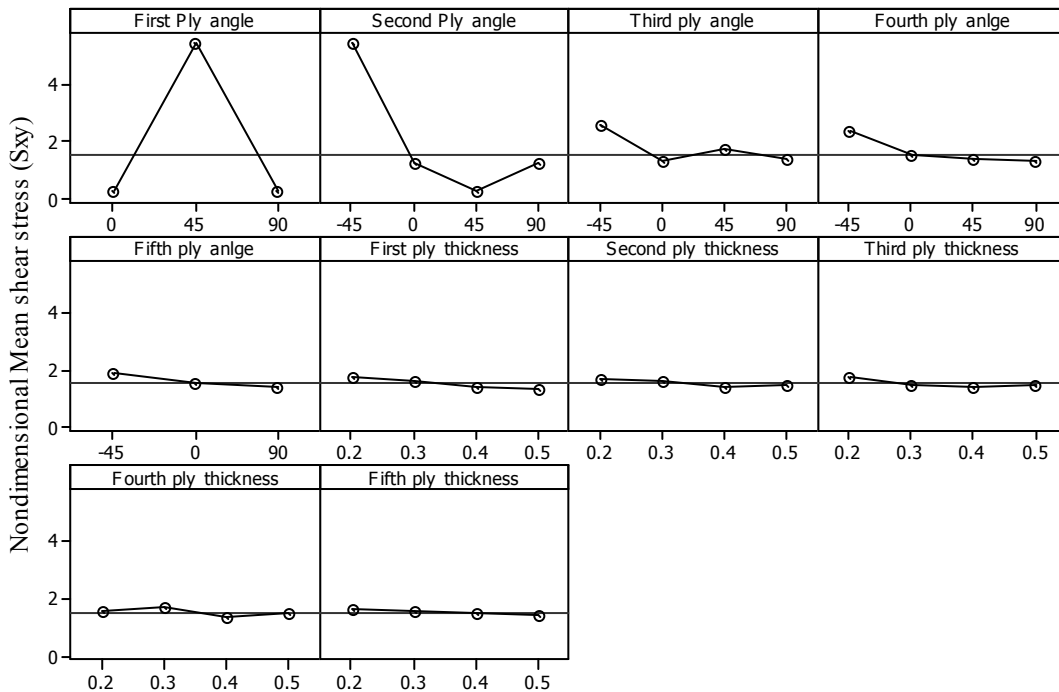


Figure 7. Variation of mean nondimensional stress (Sx) for different fibre orientations and thickness



**Figure 8.** Variation of mean nondimensional stress ( $S_y$ ) for different fibre orientations and thickness



**Figure 9.** Variations of mean nondimensional shear stress ( $S_{xy}$ ) for different fibre orientations and thickness

## 4. Results and discussion

### 4.1. Development of ANN model

One of the key issues when designing a particular neural network is to calculate proper weights for neuronal activities. These are obtained from the training process applied to the given neural network. To that end, a training sample is provided, i.e. A sample of observations consisting of inputs and their respective outputs. The observations are fed to the network. In the training process the algorithm is used to calculate neuronal weights, so that the root mean squared error between the calculated outputs and observed outputs from the training set is minimized [17].

### 4.2. Neural network training

To calculate the connection weights, a set of desired network output values is needed. Desired output values are called the training data set. The training data set in this study was selected based on a *D-optimal design* in the design of experiments. In this study, 322 data sets were used for training, 80 data set were for validation and 20 data set were used for testing the network respectively. For calculation of weight variables, often referred to as network training. To get the best prediction by the network, several architectures were evaluated and trained using the finite element analyses data. A network with one hidden layer and 30 neurons provided to be an optimum ANN. The performance of the network (RMSE and Regression coefficient ( $R^2$ )) with the number of neurons is shown in Figure 10-17. The optimal neural network architecture 10-30-4 was used in this study. It was designed using JMP software of SAS. The network consists of one input, one hidden and one output layer. The input layer has 10 neurons, hidden layer has thirty neurons and output layer has four neurons respectively. Since deflection and stresses prediction in terms of ply orientation and thickness of each ply was the main interest in this research, neurons in the input layer corresponding to the number of plies and thickness of each ply and the output layer corresponds to deflection and stresses. The minimum root-mean square error for deflection and stresses are 0.009797, 0.277487, 0.235952, and 0.049341 respectively for the training data set.

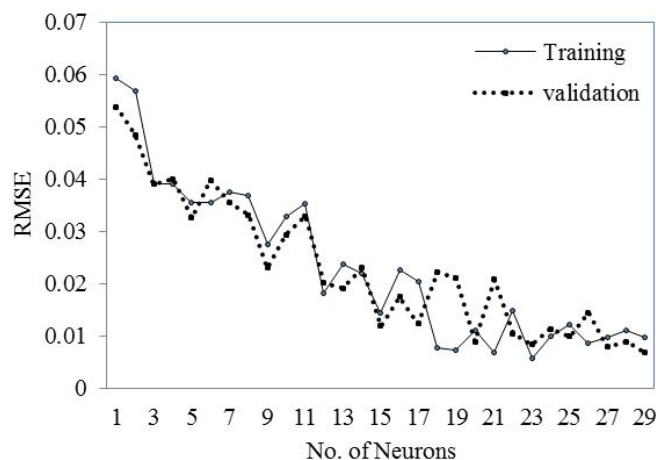


**Figure 10.** Root-mean square vs. number of neurons for nondimensional displacement

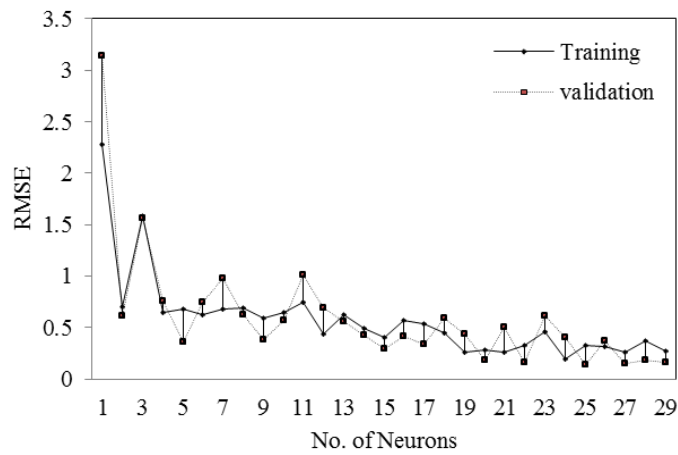


**Figure 11.** Root-mean square vs. number of neurons for nondimensional stress ( $S_x$ )

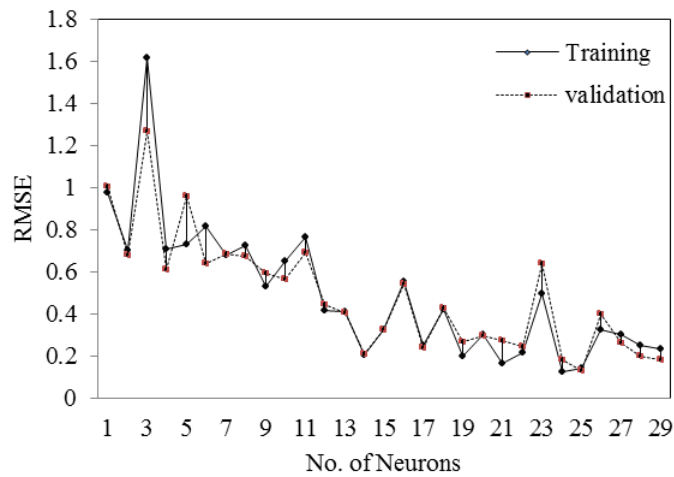


**Figure 12.** Root-mean square vs. number of neurons for nondimensional stress ( $S_y$ )

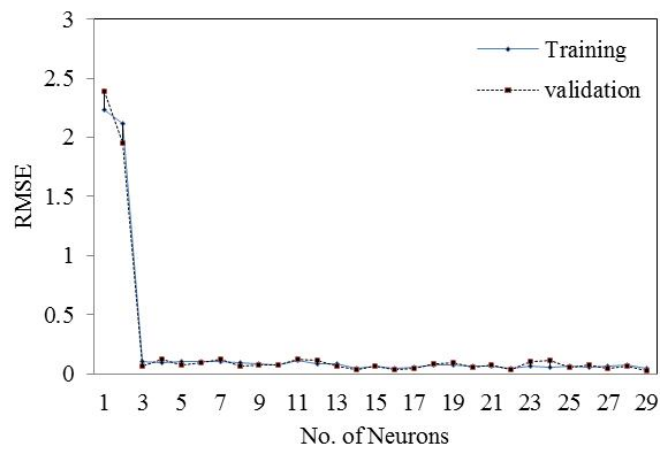


**Figure 13.** Root-mean square vs. number of neurons for nondimensional shear stress ( $S_{xy}$ )

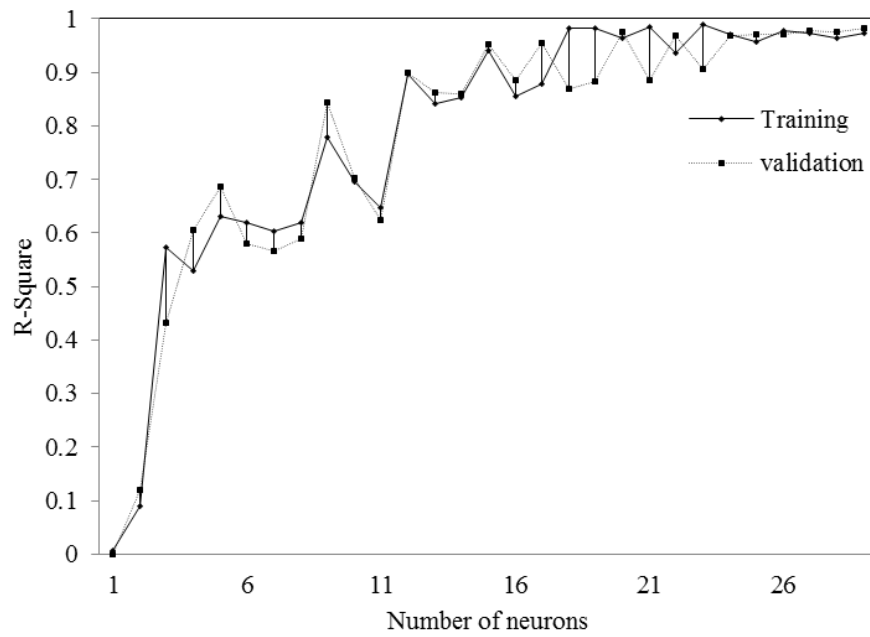


Figure 14. R-square vs. number of neurons for nondimensional deflection

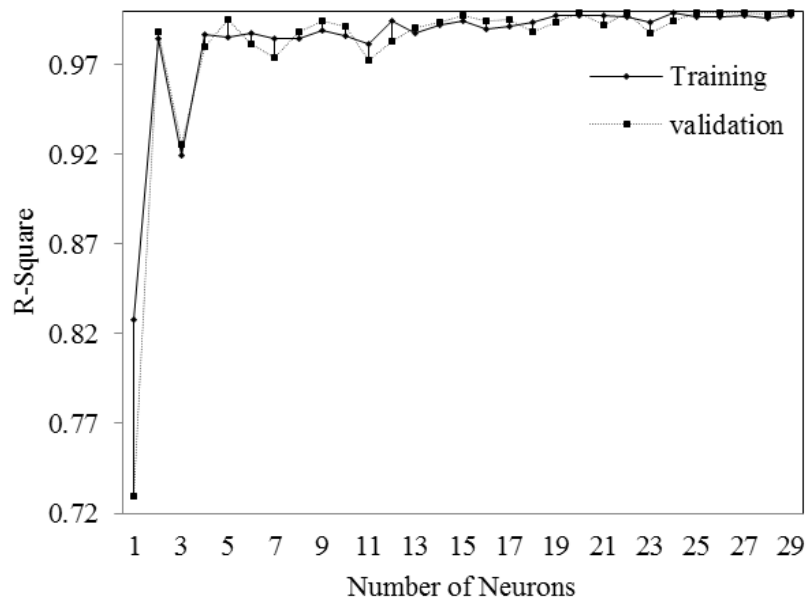


Figure 15. R-square vs. number of neurons for nondimensional stress ( $S_x$ )

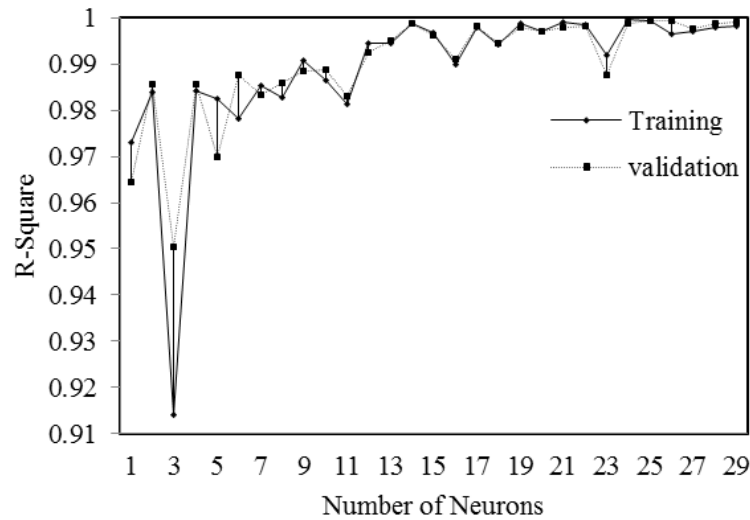


Figure 16. R-square vs. number of neurons for nondimensional stress (Sy)

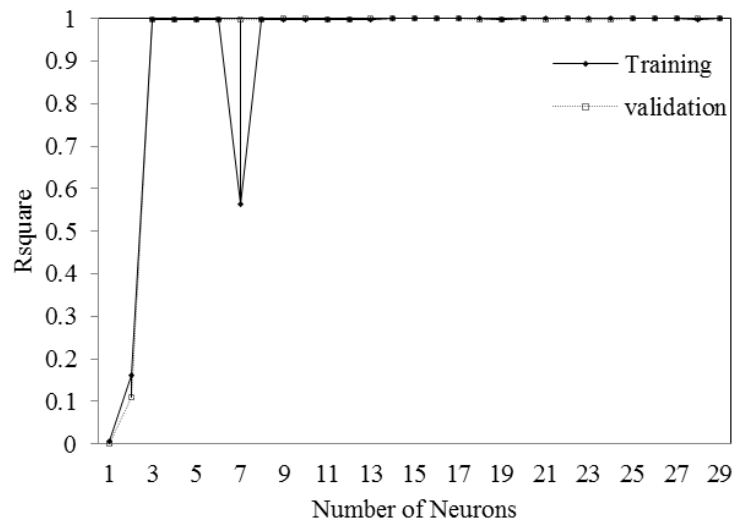


Figure 17. R-square vs. number of neurons for nondimensional shear stress (Sxy)

### 4.3. Neural network validation

Once the weights are adjusted the performance of the trained network was validated and tested with the finite element analyses which were never used in the training process. Validation set is a part of the data used to tune the network topology or network parameters other than weights. It is used to define the number of hidden units to detect the moment when the predictive ability of neural network started to deteriorate. One method,  $k$ -fold cross validation, is used to determine the best model complexity, such as the depth of a decision tree or the number of hidden units in a neural network. The method of  $k$ -fold cross validation partitions the training set into  $k$  sets. For each model complexity, the learner trains  $k$  times, each time using one of the sets as the

validation set and the remaining sets as the training set. It then selects the model complexity that has the smallest average error on the validation set (averaging over the  $k$  runs). It can return the model with that complexity, trained on all of the data. In this study  $k=5$  is chosen. The minimum validation root-mean square error for deflection and stresses are 0.0067692, 0.1574362, 0.1836281 and 0.0268278 respectively. To have a more precise investigation into the model, a regression analysis of outputs and desired targets was performed for training and validation data set as shown in Figure 18-25. The R-square values for training and, validation data set are 0.973001, 0.997533, 0.998166, 0.999546, 0.98284, 0.999249, 0.998961 and 0.999831 for deflection and stresses ( $S_x$ ,  $S_y$ ,  $S_{xy}$ ).

The comparison between ANN model output and experimental output for training, validation data sets are shown in Figure 18-25 and showing that, the predicted values using ANN is in very good correlation and representation with the experimental results.

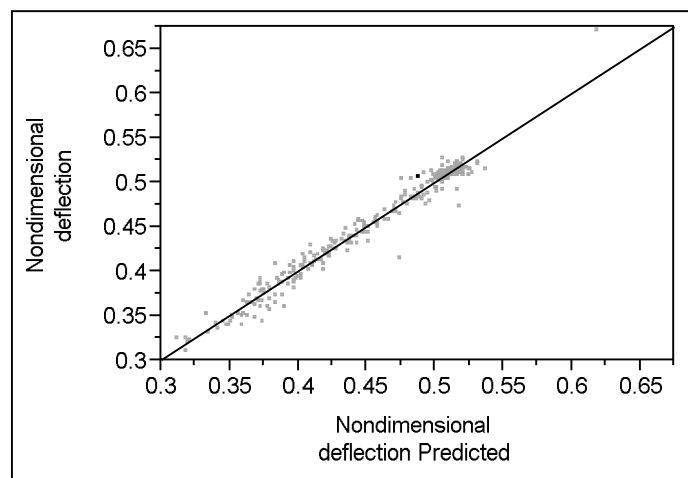


**Figure 18.** ANN predicts outputs vs. experimentally measured outputs for train data set (nondimensional deflection)

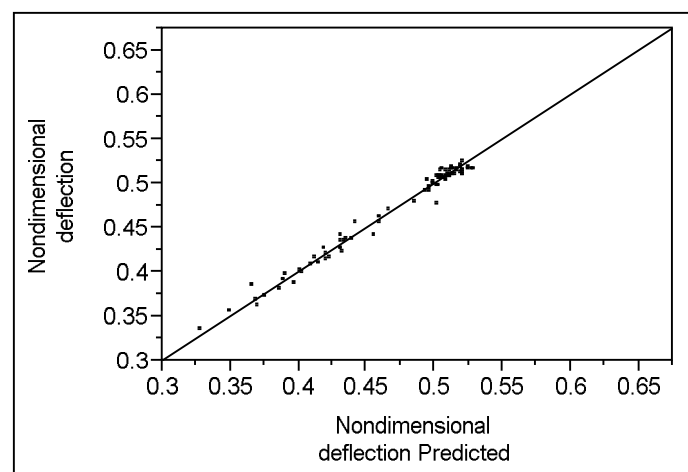


**Figure 19.** ANN predicts outputs vs. experimentally measured outputs for validation data set (nondimensional deflection)

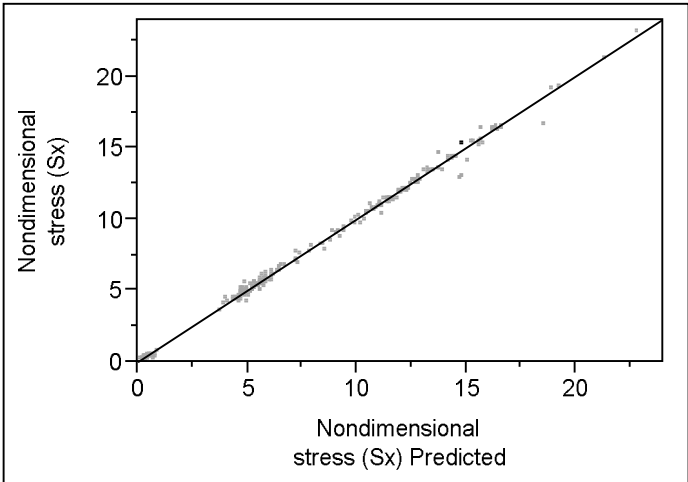


**Figure 20.** ANN predicts outputs vs. experimentally measured outputs for train data set (nondimensional stress (Sx))

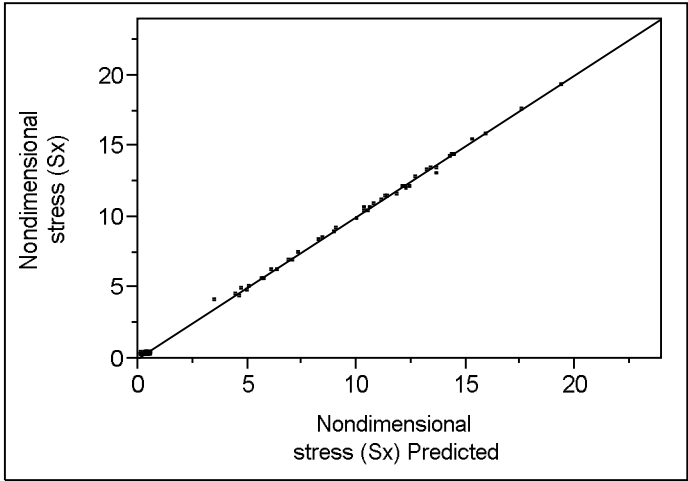


**Figure 21.** ANN predicts outputs vs. experimentally measured outputs for validation data set (nondimensional stress (Sx))

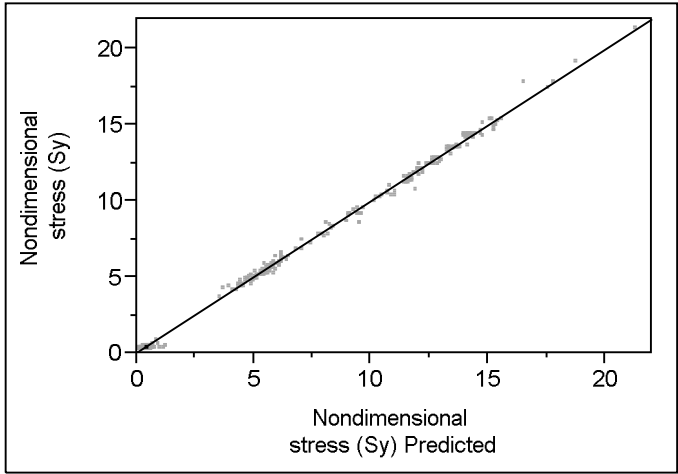


**Figure 22.** ANN predicts outputs vs. experimentally measured outputs for train data set (nondimensional stress (Sy))



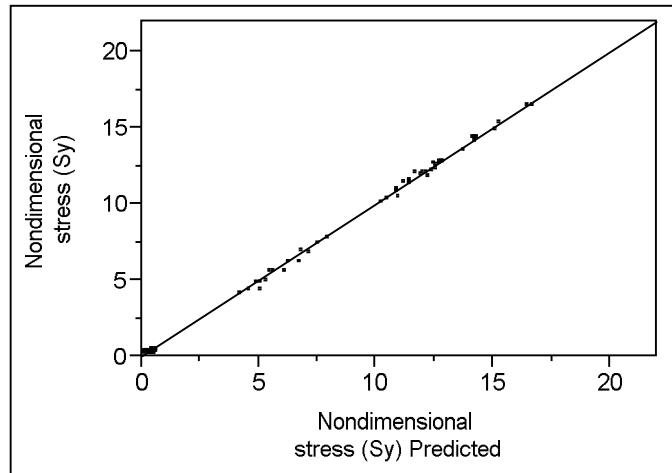


**Figure 23.** ANN predicts outputs vs. experimentally measured outputs for a validation data set (nondimensional stress ( $S_y$ ))

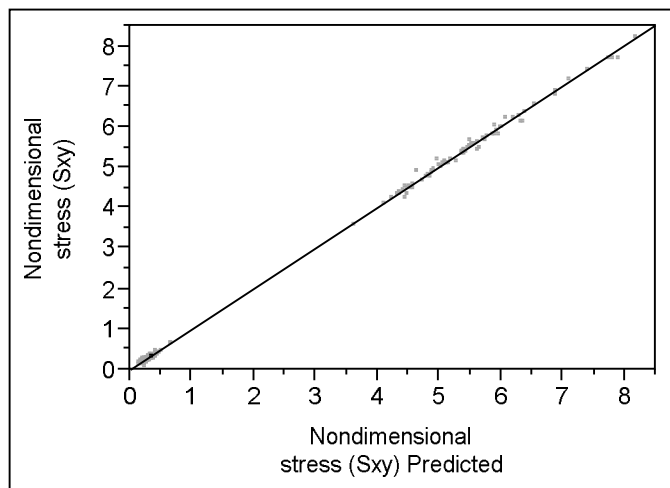


**Figure 24.** ANN predicts outputs vs. experimentally measured outputs for train data set (nondimensional stress ( $S_{xy}$ ))

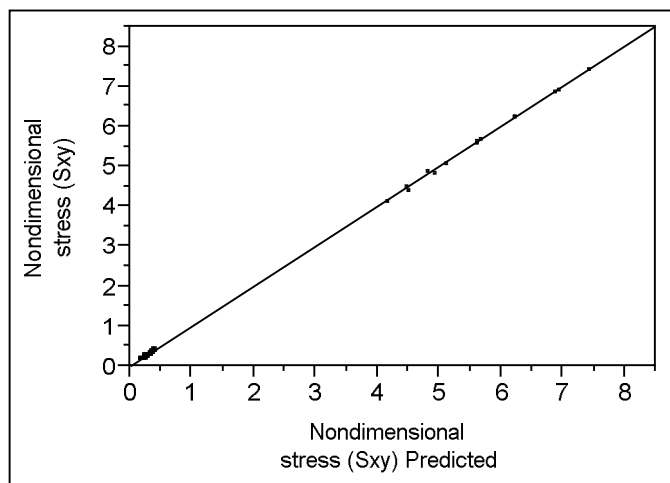


**Figure 25.** ANN predicts outputs vs. experimentally measured outputs for a validation data set (nondimensional stress ( $S_y$ ))

#### 4.4. Neural network testing

The ANN predicted results are in very good agreement with experimental results and the network can be used for testing. Hence the test data sets are applied to the network, which were never used in the training process and is presented in Table 3. The test set is a part of the input data set used only to test how well the neural network will predict on new data. The results predicted by the network were compared with the finite element results and shown in Figure 26-29. The regression coefficients for deflection and stresses ( $S_x$ ,  $S_y$ ,  $S_{xy}$ ) were found to be 0.882, 0.983, 0.993 and 0.999 respectively.

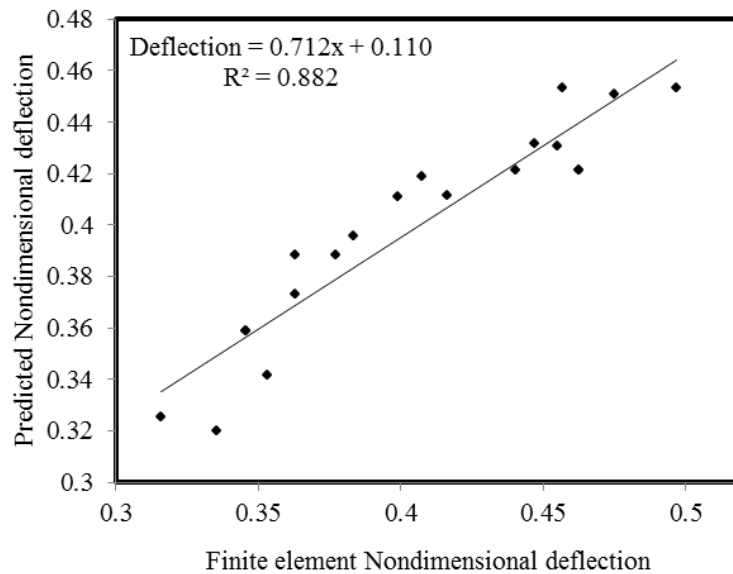


**Figure 26.** ANN predicts outputs vs. experimentally measured outputs for the test data set (nondimensional deflection)

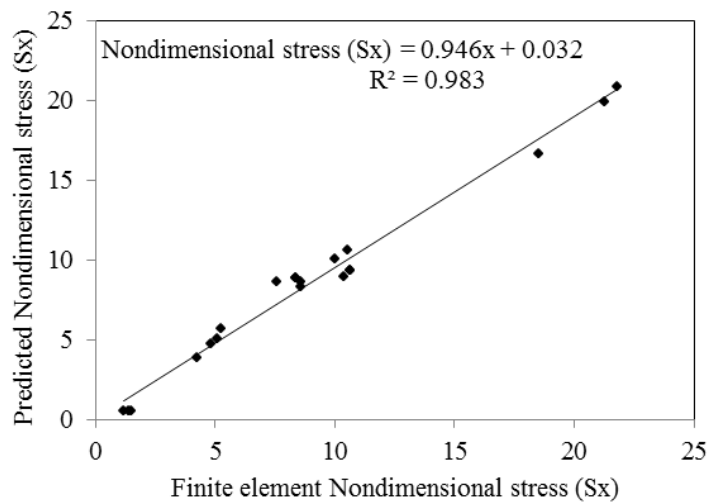


**Figure 27.** ANN predicts outputs vs. experimentally measured outputs for the test data set (nondimensional stress ( $S_x$ ))

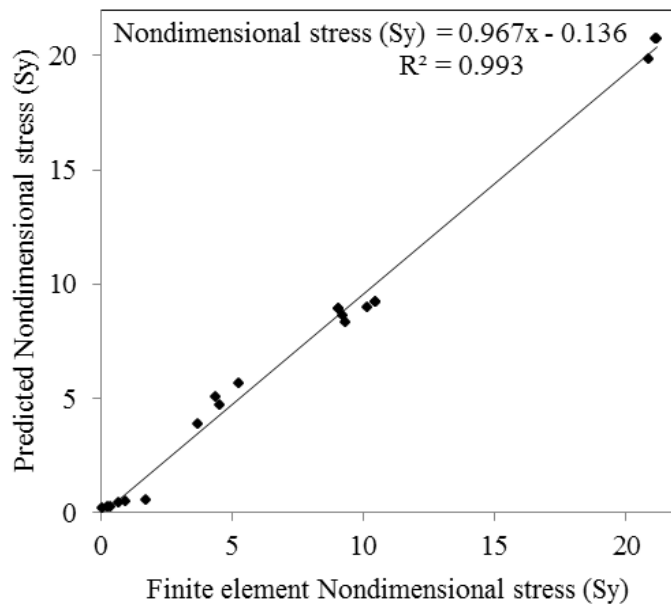


**Figure 28.** ANN predicts outputs vs. experimentally measured outputs for the test data set (nondimensional stress (Sy))

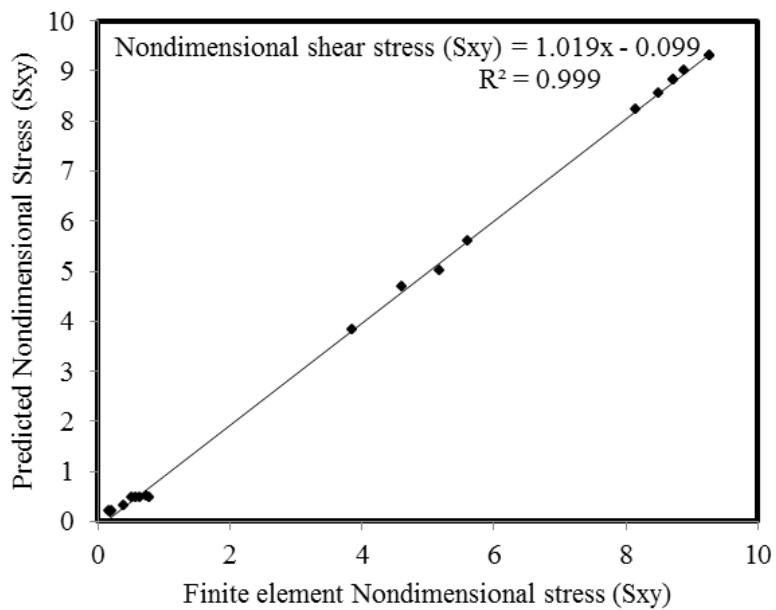


**Figure 29.** ANN predicts outputs vs. experimentally measured outputs for the test data set (nondimensional shear stress (Sxy))

Table 3. Test data set

S. No	First Ply angle	Second Ply angle	Third Ply angle	Fourth Ply angle	Fifth Ply angle	First Ply thickness	Second Ply thickness	Third Ply thickness	Fourth Ply thickness	Fifth Ply thickness
1	45	-45	45	0	-45	0.2	0.2	0.2	0.2	0.2
2	90	0	45	0	-45	0.2	0.2	0.2	0.2	0.2
3	0	90	45	0	-45	0.2	0.2	0.2	0.2	0.2
4	90	90	45	0	-45	0.2	0.2	0.2	0.2	0.2
5	45	0	90	0	-45	0.2	0.2	0.2	0.2	0.2
6	0	45	90	0	-45	0.2	0.2	0.2	0.2	0.2
7	90	45	90	0	-45	0.2	0.2	0.2	0.2	0.2
8	45	90	90	0	-45	0.2	0.2	0.2	0.2	0.2
9	45	0	-45	45	-45	0.2	0.2	0.2	0.2	0.2
10	0	45	-45	45	-45	0.2	0.2	0.2	0.2	0.2
11	45	-45	0	45	-45	0.2	0.2	0.2	0.2	0.2
12	45	90	90	0	-45	0.2	0.2	0.2	0.2	0.2
13	45	0	-45	45	-45	0.2	0.2	0.2	0.2	0.2
14	45	-45	90	45	-45	0.4	0.5	0.4	0.3	0.2
15	0	45	-45	90	90	0.4	0.5	0.4	0.2	0.2
16	0	45	-45	90	90	0.5	0.2	0.5	0.2	0.4
17	45	-45	90	0	90	0.4	0.2	0.5	0.5	0.4
18	45	0	-45	90	90	0.5	0.5	0.5	0.5	0.5
19	0	45	-45	90	90	0.3	0.4	0.5	0.3	0.4
20	45	90	-45	90	90	0.2	0.5	0.5	0.2	0.5

## 5. Conclusions

This study presented a new D-optimal set of laminates to model the artificial neural networks for predicting the deflection and stresses. The ANN predicted results are in very good agreement with the finite element results. Hence, the D-optimal design of experiments can be applied to any structural analysis. The D-optimal set of laminates is not limited to 10 ply laminates for changing the ply thickness. It is applicable to laminates of any number of plies by changing the ply thickness. The effectiveness of the method is shown with predicting capability to deflection and stresses of laminated composite plates subjected to uniformly distributed load under simply supported boundary condition.

## References

- [ 1] Akira, T. and Ishikawa, T. 2004. Design of experiments for stacking sequence optimizations with genetic algorithm using response surface approximation. *Journal of Composite Structures*, 64: 349-357.
- [ 2] Cristovao, M., Soares, M., Carlos, A., Soares, M., Victor, M., and Correia, F. 1997. Optimization of multilaminated structures using higher order deformation models. *Journal of Computational Methods in Applied Mechanical Engineering*, 149:133-152.
- [ 3] Choudhary, S. S. and Tungikar, V. B. 2011. A simple finite element for nonlinear analysis of composite plates. *International Journal of Engineering Science and technology*, 3(6): 4897-4907.

- [ 4] Ganapathi, M., Polit, O., and Touratier, M. 1996. AC0 eight-node membrane shear-bending element for geometrically non-linear (static and dynamic) analysis of laminates. *International Journal of Numerical Method in Engineering*, 39(20): 3453-3474.
- [ 5] Wanmin, H., Maurice, P., and Hsiao, Kuo-Mo. 1994. Investigation into a geometrically nonlinear analysis of rectangular laminated plates using the hierarchical finite element method. *International Journal of Finite Element Analysis and Design*, 18(1-3): 273-288.
- [ 6] Zhang, Y. X. and Kim, K. S. 2005. A simple displacement-based 3-node triangular element for linear and geometrically nonlinear analysis of laminated composite plates. *International Journal of Computational Methods in Applied Mechanical Engineering*, 194: 4607-4632.
- [ 7] Zhang, Y. X. and Kim, K. S. 2004. Two simple and efficient displacement-based quadrilateral elements for the analysis of composite laminated plates. *International Journal of Numerical Methods in Engineering*, 61: 1771-1796.
- [ 8] Zhang, Y. X. and Kim, K. S. 2006. Geometrically nonlinear analysis of laminated composite plates by two new displacement-based quadrilateral plate elements. *Journal of Composite Structures*, 72(3): 301-310.
- [ 9] Rajasekhara Reddy, M., Sidda Reddy, B., Nageswara Reddy, V., and Sreenivasulu, S. 2012. Prediction of Natural Frequency of Laminated Composite Plates Using Artificial Neural Networks. *Engineering*, 4(6): 329-337.
- [10] Shifeng, W., Wuzhu, Y., Jianxiong, K., Jun, L., and Zhufeng, Y. 2010. Simulation of the creep damage behavior of thin film/substrate systems by bending creep tests. *Journal of Materials & Design*, 31(7): 3531-3536.
- [11] Shifeng, W., Wuzhu, Y., Jianxiong, K., and Zhufeng, Y. 2010. Simulation of the interface characterization of thin film/substrate systems using bending creep tests. *Journal of Applied Surface Science*, 257(4): 1289-1294.
- [12] Ramanjaneya Reddy, A., Sidda Reddy, B., and Vijaya Kumar Reddy, K. 2011. Application of design of experiments and artificial neural networks for stacking sequence optimizations of laminated composite plates. *International Journal on Engineering, Science and Technology*, 3(6): 295-310.
- [13] Baker, A., Dutton, S., and Kelly, D. 2004. "Composite Materials for Aircraft Structures". 2nd Edition. American Institute of Aeronautics and Astronautics, Inc.1801, Chapter 8, pp. 240.
- [14] ANSYS, 2010. "Theory manual".
- [15] Reddy, J. N. 1997. "Mechanics of Laminated Composite plates". CRC Press. Florida.
- [16] Montgomery, D. C. 2001. "Design and analysis of Experiments". Fifth ed., Wiley. New York.
- [17] Principe, J., Lefebvre, C., Lynn, G., Fancourt, C., and Wooten, D. 2005. "Neurosolutions documentation". NeuroDimension, Inc.: Gainesville, FL.